Analysis of Silicon Mach Zehnder Modulator with Plus-Shaped PN Junction Phase Shifter design for Data Centre Applications

R.G. JESUWANTH SUGESH[1*], A. SIVASUBRAMANIAN[2]
[1*]ResearchScholar, Vellore Institute of Technology, School of Electronics Engineering, Chennai, INDIA,
[*]Email: jesuwanthsugesh.rg2016@vitstudent.ac.in
[2]Vellore Institute of Technology, School of Electronics Engineering, Chennai, INDIA

Abstract—Nowadays, photonic devices measuring is the investigation of interest to satisfy the development of dangerous requirements at data centres. The phase shifter (PS)performance is computed the modulator performance. In this manuscript, the plus-shaped PN junction PS is deemed. This modelis enhanced the modulation efficiency (ME)as well as decreased optical loss for higher-speed data rate (DR). To get greater efficiency of modulation, the P doped region width andthe thicknessof doped regions aredifferunder slabs. The simulation analysis of circuit-level is executed in the proposed PSacquired at travelling wave electrode (TWE) silicon Mach Zehnder modulator (SMZM). In 80 Gbps, the 12.39 dB maximal extinction ratio along 8.67×10-8 bit error rate (BER) was acquired in VπLπ of 1.05 V.cm for 3.5 mm PS length. The measured intrinsic 3 dB bandwidth denotes ~38 GHz,whereas energy per bit transmission denotes 1.71pJ/bit. More examinesare carried out to recognize the maximal communication distance using proposed PS under SMZM for the requirements of data centre.

Keywords—PN junction PS, SMZM, bit error rate, silicon photonic device, data centre.

1. Introduction

Technological advances,like5G,Internet of Things (IoT), Artificial Intelligence (AI) have leaded the way for increasing internet traffic (IT). IT is developingin alarm rate owing toenhance the file sharing, video calls and streaming, online conferences etc [1]. This increasing IT has force on data centres to implementsuchdemands. The union of international telecommunication has issued procedures governing the use of optical bandwidth. The technology of Silicon photonics (SiPh) is suggestedto fulfil the requirement of futuristic network. SiPhoffers a cost-effectual modefor incorporating the electronic with photonic modulesat Si chip by the benefits of CMOS fabrication technology [2] & [3].

The optical modulator is a noteworthy partfor higher-speed data transmission connection amid theelectronic and optic mechanisms [4 -6]. Materials along hybrid optical modulators, viz Indium Tin Oxide [7 - 13] offer maximal proficiency of modulation, but it is not compatible CMOS fabrication like silicon. At silicon optical modulators , the modulation imitates the major plasma scattering effect. In the doped region, a carrier concentration is caused by external voltage bias that leads to effectual difference of index [14].The carrier injection(CI) and carrier depletion (CD) are occurred through forward and reverse bias voltage respectively, which is utilized the standard plasma scatteringstrategies. Lesser 3dB bandwidth is a major drawback of CI strategy, because maximal capacity of dispersion junction, long lifespan of free-carrier, acquiredmaximal ME (low VπL) [4]. The CDstrategyhandles this shortcoming, also aids higher-speed data process [15] & [16]. The drawback of CD is lessME (high VπL). The obtainable Mach Zehnder modulator (MZM) is chosento its thermal stability, simple fabrication, and higher efficiency amid the optical modulators. Consuming maximal power with huge footprint is the drawback of MZM [17].

The efficiency of modulatordepends uponthe effective of PS utilizing doping pattern and concentration. By utilizing doping pattern, the PS is categorizedas interleaved, horizontal, vertical [18 – 25]. Multi-PN junctionincluding PS length presentsgreater modulation proficiencyat interleaved type PS but infabrication complexity cost. Horizontal type PS reduced the fabrication complexity, then used lesser doping concentration in PS length cost. The PS length is lessened in vertical type depending on high doping concentrated vertical slabs. Along the carrier concentration increment, increases the free carrier absorption loss.Slot like structures are employed [26 – 28] to loss minimize, but maximize the interaction of light-object. TWE is selectedon combinedstructure, owing to its independent of RC time stable. It helps CD technique [29–31] for getting huge footprint.

Through diminishing the doping region, the merits of horizontal with vertical mode doping is utilized at PS. Therefore, in this manuscript, a plus-shaped PN junction PS modelalonghigherME is proposed. The device structure is delineated in segment II. The aim is to create an optimumCD type plus-shaped PSincludinglesser VπL. Silicon MZM including proposed PS cansatisfy the higher-speed data transmission requirement on the applications of inter with intra data centre. The experimentaloutcomes have beenassessed in segment III.

2. Device Structure

Rib waveguide and 500nm width (W_{rib}), thick of ridge 220nm (t_{rib}), 90nm etching deepnesshas beendeemedbecause it providesgood optical confinement along the functioning of single-mode (TE_1), also this is a standards of fabrication.

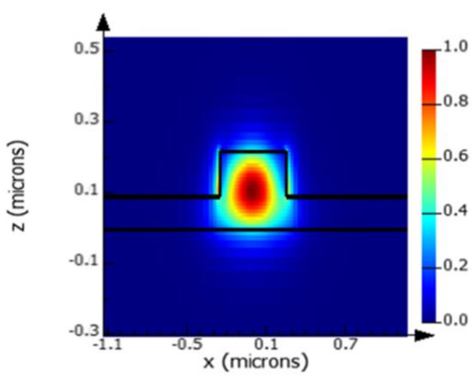

Figure 1: propagation of lightvia rib waveguide (500 × 220 nm)

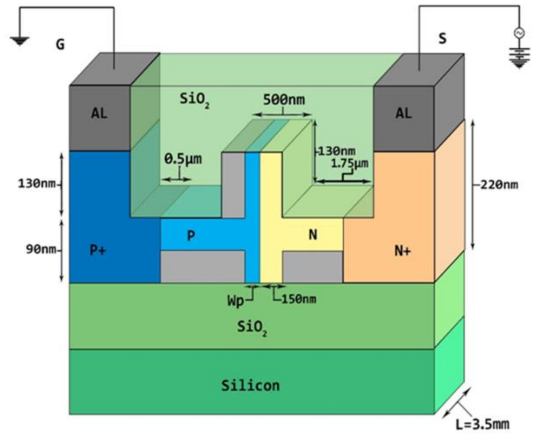

Figure 2: 3 dimensional view of plus-shaped PS

The simulation is carried out in analytical mode [32]. Figure 1 depicts the light propagation viarib waveguide.From the waveguide centre 100nm offset is imitated to PN junction for improving the efficiency of phase. The N doped region width is set as 150nm, thickness of (P, N) slabs set as70nm. The concentrations of P as well as N doped set to 9×10^{17} cm^{-3} and 7×10^{17} cm^{-3}, becauseholes contain huge shift index with lesser absorb than electrons [7]. At the edge of waveguide, slab resistance has been diminished to 1×10^{19} cm^{-3} carrier concentration of P+ together with N+ doped region. Aluminium electrodes (Al) have been employed into electrical contacts. The PS (L) lengthis set as 3.5mm. Figure 2 depicts 3 dimensional view of plus-shaped PS. Maximal 5 V driving voltage is utilized to cathode (V = 0 to 5V) for maintainingminimal power consumption.

3. Result Analysis

The analysis was categorizedas 2level simulation: (i) device(ii) system (Figure 3). On device-state, the electro-optic as well as RF behaviour of PSis carried outwith the help of finite-difference eigenmode (FDE) evaluation (Figure 3.a). In system-level, the PS parameters design is derivedfrom MZM (PS-MZM) in Lumerical Interlink (Figure 3.b). The long-distance transmission as well as higher-speed DRis implementedfor examining the proficiency of PS-MZM’s tothe application of data centre on and off-chip transmission.

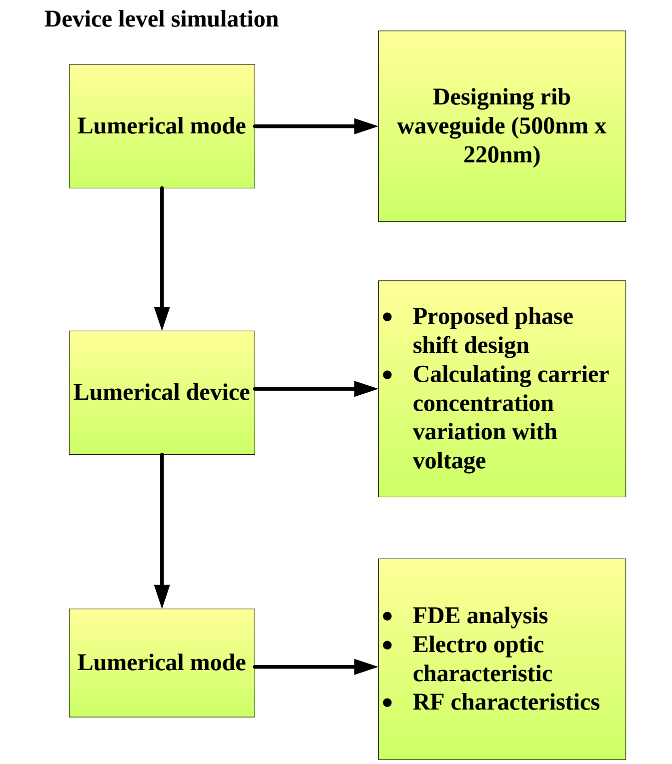

Figure 3:Simulation flow for result analysis (a) Device-level simulation

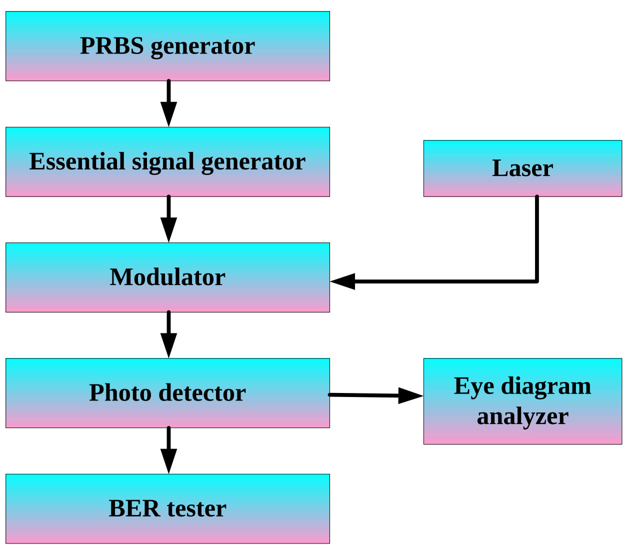

Figure 3: Simulation flow for result analysis (b) System-level simulation

3.1 Assessment of Device level

The reverse bias voltage(BV) of PSis variesfor analysing the electro-optic PS performance. When BVis maximized, the carriers have beendepletion from PN junction. It diminishes thedensity of carrier,sodiminished the junction capacitancethat is represented at Figure 4. The junction capacitance (C) depending upon electron (N_n),density (1), hole (N_p).

$$C = \frac{t_{rib} \times \sqrt{(q\varepsilon_0\varepsilon_r)}}{\sqrt{(2(N_p{}^{-1} + N_n{}^{-1}) \times (V_v - V))}} \quad (1)$$

Here, q implicates electric charge,ε_0 specifies dielectric constant, ε_r as relative permittivity, V_v as dispersion capacity.

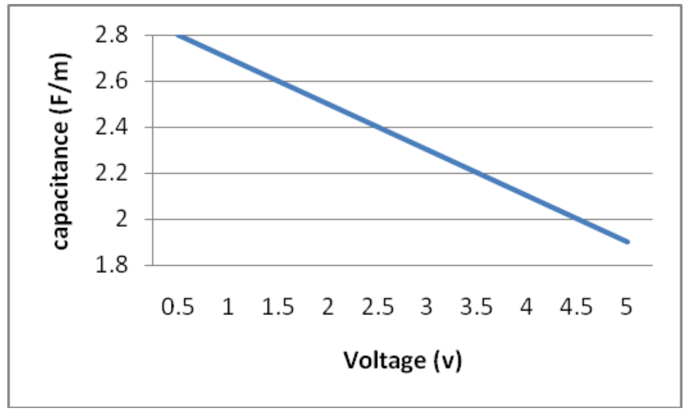

Figure 4: Junction Capacitance ofPS for varying BV

CDis the impact of refractive index (Δn), absorption coefficient $(\Delta\alpha)$of PS. The derivation (2) and (3)is exhibited by Soref and Bennett [14].

$$\Delta n = -8.8 \times 10^{-22} N_n - 8.5 \times 10^{-18} N_p{}^{0.8} \quad (2)$$

$$\Delta\alpha = 8.5 \times 10^{-18} N_n + 6 \times 10^{-18} N_p \quad (3)$$

The optical PS feature is modified by effectual index change (5) and voltage ($\Delta n_{eff}(V)$). It occurs phase shift (φ) at propagating optical wave (OW)includingPS length(L),which is exhibited in (6).

$$n_{eff}(V) = n_{eff,i} + \int \Delta n(V) dV$$
(4)

Here, $n_{eff,I}$implies effectual waveguide index without doping.

$$\Delta n_{eff}(V) = n_{eff}(V) - n_{eff}(0) \quad (5)$$

$$\varphi(V) = \frac{2\pi \Delta n_{eff}(V)}{\lambda L} \quad (6)$$

The absorption coefficientα with PS (z-axis) is ,

$$\alpha(k) = \frac{\iint \Delta\alpha(V)|E(x,y,z)^2| dxdy}{\iint |E(x,y,z)^2| dxdy} \quad (7)$$

Here, x, y impliescoordinates of waveguide dimension, z specifies length coordinate of PS, $E(x,y,z)$signifies waveguide mode optical supply of intensity.

The absorption loss(AL) is the noteworthy part of overall loss in PS. Owing to the photons absorption via carriers, the AL is occurred (free carrier loss of absorption). As the voltage increases, the carriers drop from the junction, it lessens the carrier AL with PS. (Figure 5). The free carriers are higherwhile P doped region (Wp) is huge,so the loss is higherviaPS is acquired in lesser voltages. If the region of P doped is tiny,then decreases the loss.The necessary PSderived inmaximal voltage owing to lesser variation of carrier concentration.It derives Wp= 100nm a minimal loss, then needed πPS is acquired within the limits of voltage set. If diminishing Wp<100nm, then the loss diminishesin the cost of phase efficient. The necessary PSto modulation is derived in 3.05V (Vπ) reverse bias voltage atpresented structure along 4.1 dB loss. Figure 6 depicts the Vπ differenceincluding loss ofPS length operation. Vπ lessens the propagationOWhas visiblefor change thePhase shiftof entirePS length with maximizing length.If maximizing the carriers communication, optical mode, length, then maximizes the loss, length, but minimizes the speed ofoperating. It creates trade-off stage amid theVπ and PS distance.

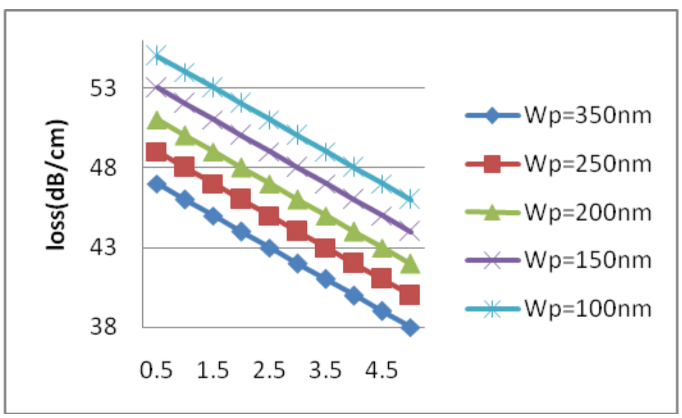

Fig 5: Loss Vs voltage to vary Wp at the presented design

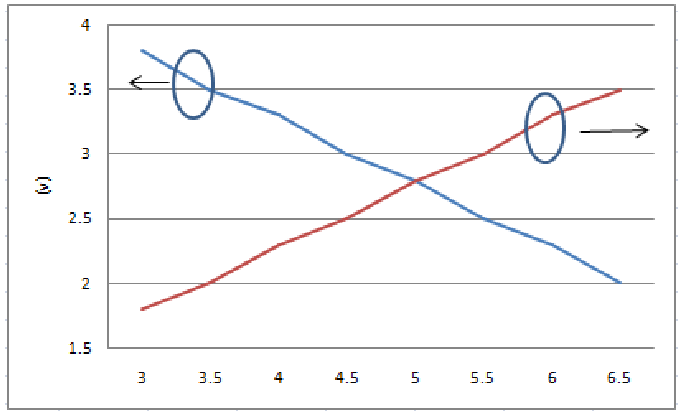

Figure 6: Vπ including loss variation depending onPS length for proposed PS design along Wp = 100nm

The 3dB intrinsic bandwidth ($f_{3dB} = \frac{1}{2\pi RC}$) of PS is determined as 37.7GHz. Here, TWE is suggested for dealing the stable RC time, thenstrongly connect the RF microwave includingOW. To robust connect, optical group index (OGI) must be equivalent to effectual index in specific frequency. In 26GHz, assume the index match, it leads to maximal link amidthemode of RF and optical. Figure 7 portrays the loss of 3 dB/cm determinesin 26GHz.Here, loss is directly proportional to the frequency of microwave. To 3.5mm length design, 6dB bandwidth of 24.75GHz is reached(Figure 8), alsoassures that the device isdeemed to the communication of higher-speed DR.

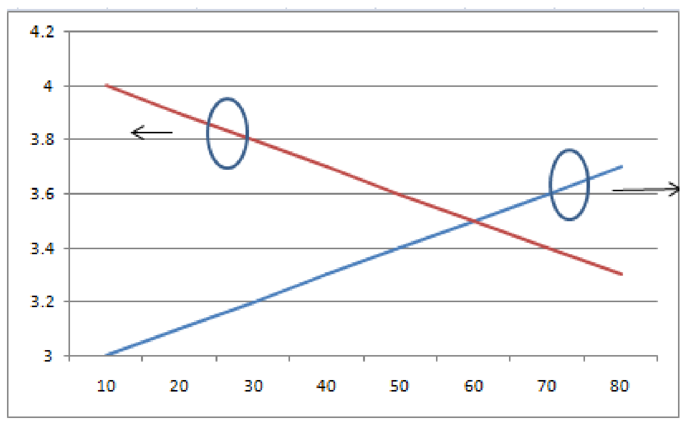

Figure 7: RF effectual index with Loss obtaineddepending on frequency

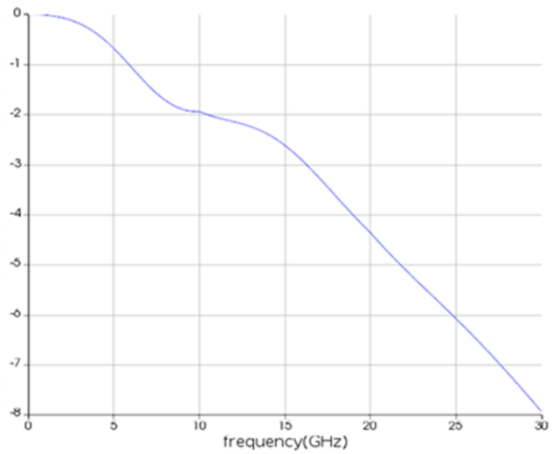

Figure 8: Electrical S21 (dB) utilizing frequency

3.2 System-level performance

Here, the dynamic performance of imbalanced MZM combinedtoPSdesign is described. PS-MZM contains 100µmdeliberate length dissimilarityincluding long arm, whichprovides 0.5V fixed bias voltage as well asirregular voltage swing (V_{pp}) and direct current reverse bias (V_{dc}) are employed toanother arm. At 80Gbps,the generator of pseudo-random bit sequence (PRBS) createsa communication data. The electrical signal producerand NRZ line coding method were utilized for converting logical data as electric signalmessage. The 1552.5nmcarrier signal is created byCW Laser. Demodulate the acquired modulated signal utilizing photodetector responsivity and 1A/W. BERincluding eye diagram isassess the signal of demodulated. Here, 12.39dBfor eye diagram including extinction ratio (ER), 8.67×10^{-8} for BER, 1.05V.cmfor VπL attains $3V_{pp}$, $1.5V_{dc}$. The eye-crossing is approximately 50% as well as broad eye opening guides to the deviation of minimal duty cycle with minimal inter-codeinterfering. It assures the PS-MZM is appropriate for higher-speed DRutilizations. The usage of energy per bit ($E_{bit} = \frac{CV^2}{4}$)todata transfer is determined as 1.71pJ/bit. The proficiency of presented method is likened to the published articles result that is tabulated in Table 1.

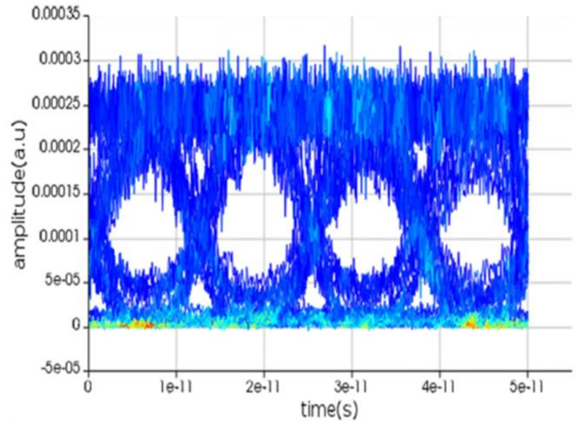

Figure 9: Eye diagram of PS-MZM and VπL = 1.05V.cm

Table 1: Published result's parameter comparison

Ref	L (mm)	Gbps	VπLπ (V.cm)	ER (dB)
[19]	0.75	40	1.5	7.01
[20]	8	-	3.1	18
[23]	1.5	112	2.3	-
[24]	5	100	2.5	5.5
[25]	3	10	1.08	11
[26]	1.2	100	0.74	2.4
This work	3.5	80	1.05	12.3

Greater ER is derived [20] through raising the length of PS. At [24], 5mm PS length has been utilized forgetting the π phase shift and 5.5dB ER.Diminished the length to 1.2 mm [27] but requires the reverse BVapproximately 6V, also 2.4dB of ER has been acquired. Table1 displays thePS in MZM works excellentlikened todifferent published outcomes.

Upto 15km length ofdata centres span have beenlinked through fibre optic cables. The PS-MZM efficacy to communicateamid chips coupledutilizing fibre optic cables. In 80Gbps, λ = 1552.5nm, the proficiency of transmission distance is assessed. Figure 9 represents forward error correction (FEC) threshold of bit error rate 1×10^{-3} (among chips) that PS-MZM couldtransfer upto 29km. It assures PS-MZM is appropriateto intra data centre utilizations alongwave transmission of guided (optical fibre) with unguided (free space optics). The transmission length is maximizedutilizing amplifier.

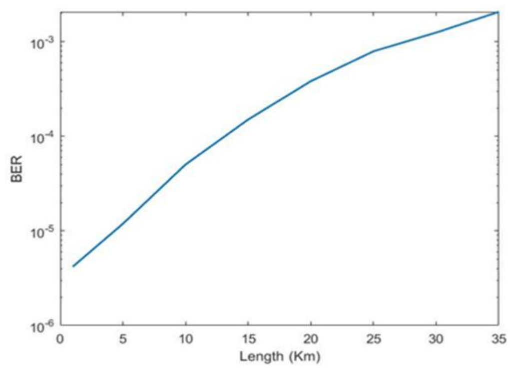

Figure 10: Transmission proficiency of PS-MZM on fibre optic cable at 80 Gbps

The speed capability of PS-MZM is deemed throughchanging the bit rate,then computes the BER. With maximizing bit rate, BER maximizes as inferred from figure 10. Here, PS-MZM aids to 95Gbps. Thebit rate isincreased by enhancing the responsivity of PIN photorecognizers or presentingthe filter.

4. Conclusion

This manuscript proposes 3.5mm length plus-shaped PN junction PSfor attaining greater efficacy of modulation. At the proposed design, P doped region width on rib attains100nm,thickness of P, N doped slab regions attains 70nm. In 80 Gbps,the PS with SMZM, an ER of 12.39 dB as well as 8.67×10^{-8} BER acquiresin 1.05 V.cm $V\pi L\pi$ for the wavelength of 1552.5 nm. The modulator is structured for fulfilling the data centre futuristic requirements,also utilized in another utilizations, viz optical switches. The PS in MZM is examinedto itsassociate distance (29 km for inter with intra data centre interlink communication without amplifier). With the help of complex modulation modes, more enhancements in bit rate is derived.

Reference

[1] E. Perspectives and C. Report, "Cisco Annual Internet Report - Cisco Annual Internet Report (2018–2023) White Paper", Cisco, 2020. [Online]. Available: https://www.cisco.com/c/en/us/solutions/collateral/service-provider/visual-networking-index-vni/white-paper-c11-741490.html.

[2] H. Subbaraman et al., "Recent advances in silicon-based passive and active optical interconnects", Optics Express, vol. 23, no. 3, pp. 2487, 2015.

[3] D. Thomson et al., "Roadmap on silicon photonics", Journal of Optics, vol. 18, no. 7, pp. 073003, 2016.

[4] Q. Xu, S. Manipatruni, B. Schmidt, J. Shakya and M. Lipson, "125 Gbit/s carrier-injection-based silicon micro-ring silicon modulators", Optics Express, vol. 15, no. 2, pp. 430, 2007.

[5] W. Green, M. Rooks, L. Sekaric and Y. Vlasov, "Ultra-compact, low RF power, 10 Gb/s silicon Mach-Zehndermodulator", Optics Express, vol. 15, no. 25, pp. 17106, 2007.

[6] L. Chen, K. Preston, S. Manipatruni and M. Lipson, "Integrated GHz silicon photonic interconnect with micrometer-scale modulators and detectors", Optics Express, vol. 17, no. 17, pp. 15248, 2009.

[7] L. Alloatti et al., "100 GHz silicon–organic hybrid modulator", Light: Science & Applications, vol. 3, no. 5, pp. e173-e173, 2014.

[8] N. Youngblood, Y. Anugrah, R. Ma, S. Koester and M. Li, "Multifunctional Graphene Optical Modulator and Photodetector Integrated on Silicon Waveguides", Nano Letters, vol. 14, no. 5, pp. 2741-2746, 2014.

[9] X. Zhang et al., "High Performance Optical Modulator Based on Electro-Optic Polymer Filled Silicon Slot Photonic Crystal Waveguide", Journal of Lightwave Technology, vol. 34, no. 12, pp. 2941-2951, 2016.

[10] J. Baek, J. You and K. Yu, "Free-carrier electro-refraction modulation based on a silicon slot waveguide with ITO", Optics Express, vol. 23, no. 12, pp. 15863, 2015.

[11] H. Dalir, Y. Xia, Y. Wang and X. Zhang, "Athermal Broadband Graphene Optical Modulator with 35 GHz Speed", ACS Photonics, vol. 3, no. 9, pp. 1564-1568, 2016.

[12] S. Rajput, V. Kaushik, S. Jain and M. Kumar, "Slow Light Enhanced Phase Shifter Based on Low-Loss Silicon-ITO Hollow Waveguide", IEEE Photonics Journal, vol. 11, no. 1, pp. 1-8, 2019.

[13] S. Rajput, V. Kaushik, S. Jain, P. Tiwari, A. Srivastava and M. Kumar, "Optical Modulation in Hybrid Waveguide Based on Si-ITO Heterojunction", Journal of Lightwave Technology, vol. 38, no. 6, pp. 1365-1371, 2020.

[14] R. Soref and B. Bennett, "Electrooptical effects in silicon", IEEE Journal of Quantum Electronics, vol. 23, no. 1, pp. 123-129, 1987.

[15] A. Liu et al., "High-speed optical modulation based on carrier depletion in a silicon waveguide", Optics Express, vol. 15, no. 2, pp. 660, 2007.

[16] M. Ziebell et al., "40 Gbit/s low-loss silicon optical modulator based on a pipin diode", Optics Express, vol. 20, no. 10, pp. 10591, 2012.

[17] R. JesuwanthSugesh and A. Sivasubramanian, "Redesigning Mach-Zehnder Modulator with Ring

Resonators", Lecture Notes in Electrical Engineering, pp. 185-191, 2017.

[18] P. Dong, L. Chen and Y. Chen, "High-speed low-voltage single-drive push-pull silicon Mach-Zehnder modulators", Optics Express, vol. 20, no. 6, pp. 6163, 2012.

[19] H. Xu et al., "High speed silicon Mach-Zehnder modulator based on interleaved PN junctions", Optics Express, vol. 20, no. 14, pp. 15093, 2012.

[20] A. Rao et al., "High-performance and linear thin-film lithium niobate Mach–Zehnder modulators on silicon up to 50 GHz", Optics Letters, vol. 41, no. 24, pp. 5700, 2016.

[21] M. Félix Rosa et al., "Design of a carrier-depletion Mach-Zehnder modulator in 250 nm silicon-on-insulator technology", Advances in Radio Science, vol. 15, pp. 269-281, 2017.

[22] T. Ang, C. Png and S. Lim, "Numerical analysis and optimization of high-speed silicon microring resonator modulators utilizing higher-performance carrier-depletion phase shifters", Silicon Photonics XII, 2017.

[23] G. de Farias, Y. Bustamante, H. de Andrade, U. Moura, A. Freitas and D. de A. Motta, "Demonstration of > 48GHz Single-Drive Push-Pull SMZM with Lower V<inf>Π</inf>L", 2018 IEEE 15th International Conference on Group IV Photonics (GFP), Cancun, Mexico, 2018, pp 1-2.

[24] M. He et al., "High-performance hybrid silicon and lithium niobateMZMto 100 Gbit s−1 and beyond", Nature Photonics, vol. 13, no. 5, pp. 359-364, 2019.

[25] K. Ogawa et al., "Silicon-based phase shifters for high figure of merit in optical modulation", Silicon Photonics XI, 2016.

[26] R. Palmer et al., "Silicon-Organic Hybrid MZI Modulator Generating OOK, BPSK and 8-ASK Signals for Up to 84 Gbit/s", IEEE Photonics Journal, vol. 5, no. 2, pp. 6600907-6600907, 2013.

[27] S. Jain, S. Rajput, V. Kaushik and M. Kumar, "High speed optical modulator based on silicon slotted-rib waveguide", Optics Communications, vol. 434, pp. 49-53, 2019.

[28] S. Jain, S. Rajput, V. Kaushik, Sulabh and M. Kumar, "Efficient Optical Modulation With High Data-Rate in Silicon Based Laterally Split Vertical p-n Junction", IEEE Journal of Quantum Electronics, vol. 56, no. 2, pp. 1-7, 2020.

[29] T. Baehr-Jones et al., "Ultralow drive voltage silicon traveling-wave modulator", Optics Express, vol. 20, no. 11, pp. 12014, 2012.

[30] J. Dakin and R. Brown, "Handbook of Optoelectronics (Two-Volume Set)", CRC press, 2006.

[31] L. Binh, Optical multi-bound solitons, 1st ed. 2015.